J|A|C|S
COMMUNICATIONS

Published on Web 12/23/2004

A Crystallographic Investigation of Phosphoantigen Binding to Isopentenyl Pyrophosphate/Dimethylallyl Pyrophosphate Isomerase

Johan Wouters,[†] Fenglin Yin,[‡] Yongcheng Song,[§] Yonghui Zhang,[§] Yamina Oudjama,[†] Victor Stalon,[†] Louis Droogmans,[†] Craig T. Morita,[∥] and Eric Oldfield*[,‡,§]

Institute de Recherche Wiame and Laboratoire de Microbiologie, Universite Libre de Bruxelles, 1 Avenue E. Gryson, 1070 Bruxelles, Belgium, Department of Biophysics, 600 South Mathews Avenue, University of Illinois at Urbana-Champaign, Urbana, Illinois 61801, Department of Chemistry, 600 South Mathews Avenue, University of Illinois at Urbana-Champaign, Urbana, Illinois 61801, and Department of Internal Medicine, University of Iowa, EMRB 340F, Iowa City, Iowa 52242

Received September 2, 2004; E-mail: eo@chad.scs.uiuc.edu

The mevalonate isoprene-biosynthesis pathway is an important target for a broad variety of drugs, such as statins,[1] anti-fungals,[2] and bisphosphonates.[3] In addition to their use in treating bone resorption diseases, bisphosphonates such as pamidronate (Aredia, **1**) have recently been found to stimulate $\gamma\delta$ T cells of the immune system.[4] The mevalonate pathway has been implicated in this process,[5] and there is currently interest in the use of bisphosphonates in immunotherapy for B cell malignancies.[6] A second set of $\gamma\delta$ T cell antigens of clinical interest are the "phosphoantigens", molecules such as the epoxides and bromohydrins of isopentenyl pyrophosphate (**2**, **3**): **2** is also known to be an inhibitor of the

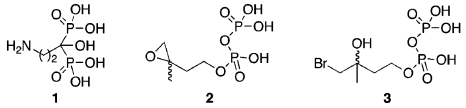

mevalonate pathway, since it alkylates the enzyme isopentenyl pyrophosphate/dimethylallyl pyrophosphate isomerase (IPPI),[7] forming a C67 thioether or a E116 ester at the C-3 position of the isoprenoid. These are key active-site residues, with E116 being thought to protonate the IPP double bond while the C67 thiolate removes a C-2 proton.[8] Here, we report that the potent phosphoantigen **3** (Phosphostim) is also an inhibitor of IPPI, forming covalent adducts with C67 and E116. This leads to a mechanistic proposal for its mode of action in IPPI inhibition.

Production, purification, and crystallization of both wild-type (w.t.) and a mutant (Y104F) IPPI were carried out as described previously in refs 8 and 9 and in the Supporting Information. The protein crystallizes with two molecules in the asymmetric unit, related by two-fold rotational noncrystallographic symmetry.[9] Full crystallographic details for all four structures determined are given in Table 1.[10]

The 1.68 Å crystallographic structure of w.t. IPPI after reaction with *rac*-**3** is shown in Figure 1 (PDB File 1PPV). *rac*-**3** binds in two ways to IPPI. In the first (Figures 1 and S1), the bromine atom is displaced by the thiol of C67, forming a 4-thioether. In the second, the bromine is displaced by the carboxylate of E116, forming a 4-ester (Figures 1 and S2). However, unlike the situation with alkylation by **2**,[8] both the thioether and the ester group form at C-4, not at C-3. In both cases, the pyrophosphate groups bind to Mg^{2+} and the K21, K55, R51, and R83 Lys/Arg cluster. In addition, H69 is weakly hydrogen-bonded to a pyrophosphate oxygen, in each system ($d_{N-O} \approx 3.0$ Å, on average).

[†] Universite Libre de Bruxelles.
[‡] Department of Biophysics, University of Illinois at Urbana-Champaign.
[§] Department of Chemistry, University of Illinois at Urbana-Champaign.
[∥] University of Iowa.

Table 1. Data Collection and Refinement Statistics

crystal	1PPV	1X83	1X84	1PPW
complex	*rac*-**3**, w.t.	*S*-**3**, w.t.	*S*-**3**,Y104F	**4**, w.t.
space group	$P2_12_12_1$	$P2_12_12_1$	$P2_12_12_1$	$P2_12_12_1$
cell index (Å)	$a = 69.1$	$a = 69.1$	$a = 69.1$	$a = 69.1$
	$b = 71.8$	$b = 71.9$	$b = 71.8$	$b = 71.9$
	$c = 92.0$	$c = 91.9$	$c = 92.0$	$c = 91.7$
wavelength (Å)	0.9292	0.9292	0.9292	1.54179
resolution (Å)	1.68	1.78	1.65	2.1
total reflections	199 126	171 333	327 874	100 391
unique reflections	55 235	44 272	56 530	21 497
observed reflections	45 724	42 813	50 029	17 878
completeness (%)[a]	97.4 (88.3)	95.9 (79.9)	99.9 (88.5)	98.4 (95.1)
R_{sym}[a,b]	4.1 (8.5)	3.6 (12.0)	4.0 (10.4)	8.8 (29.8)
I/σ[a]	21.4 (8.4)	19.3 (7.2)	15.6 (5.8)	18.7 (7.1)
R_{work}/R_{free}[c]	18.8/23.5	20.1/25.2	22.4/27.0	17.6/25.7
	rmsd from Ideal Geometry			
bonds (Å)	0.008	0.005	0.004	0.004
angles (deg)	0.024	0.022	0.022	0.019
	Ramachandran Plot			
most favored (%)	89.5	88.5	89.8	88.2
additional (%)	10.5	11.5	10.2	11.5
generously (%)	0.0	0.0	0.0	0.3
disallowed (%)	0.0	0.0	0.0	0.0

[a] Values listed in parentheses are for the highest-resolution shell. [b] $R_{sym} = \sum|I - \langle I\rangle|/\sum I$, where I is the observed intensity of a reflection and $\langle I\rangle$ is the averaged intensity of multiple observations of the reflection and its symmetry partners. [c] $R_{factor} = \sum||F_o| - |F_c||/\sum|F_o|$, where F_o and F_c are the observed and calculated structure factors, respectively. R_{free} was calculated with 10% of the reflections set aside randomly throughout the refinement.

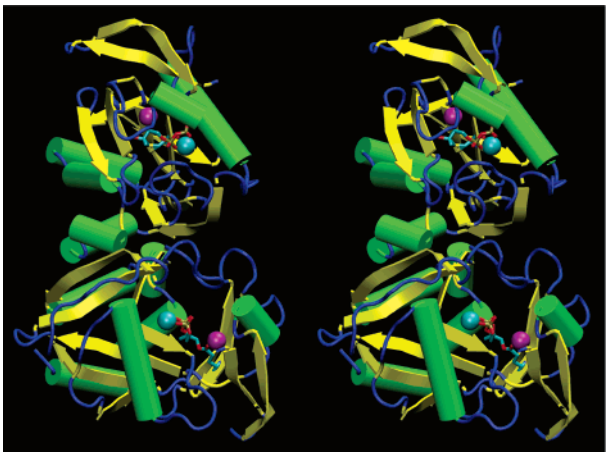

Figure 1. Stereoview for full crystal structure of *rac* **3**−IPPI (w.t. enzyme) complex (PDB File IPPV).

It is not possible from these results to determine whether both enantiomers of **3** react with the protein, since the 3-Me and 3-OH groups cannot be differentiated. We therefore produced the *S*-form

10.1021/ja040207i CCC: $30.25

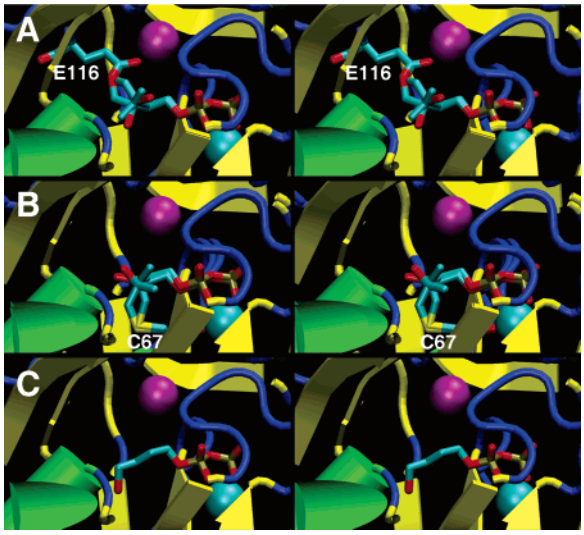

Figure 2. Stereoviews for crystal structures of **A**, *rac*-**3**−IPPI (w.t. enzyme) ester complex (PDB File IPPV) together with the *S*-**3**−IPPI (w.t. enzyme) ester complex (PDB File 1X83); **B**, *rac*-**3**−IPPI (w.t. enzyme) thioether complex (PDB File IPPV) together with the *S*-**3**−IPPI (Y104F mutant) thioether complex (PDB File 1X84); and **C**, **4**−IPPI (w.t. enzyme) complex (PDB File IPPW).

of **3**[11] and obtained its structure (PDB File 1X83) bound to w.t. IPPI (Figure S3). Only the E116 ester forms with *S*-**3**, and as shown in Figure 2A, there is close register (0.96 Å heavy atom rmsd) between the *rac*-**3** and *S*-**3** ester structures. These results suggest, then, that *R*-**3** forms the 4-thioether in the *rac*-**3** complex.

We also investigated how *S*-**3** binds to the Y104F mutant of IPPI. Y104 is also now thought to be involved (with E116) in protonating the double bond in IPP, since the Y104F mutant has only ∼10% of the catalytic activity of w.t. IPPI.[12] The crystallographic structure (PDB File 1X84) of *S*-**3** bound to Y104F IPPI (Figure S4) shows that in this case, a 4-thioether forms with C67. Remarkably, this *S*-form shows close register with the *R*-thioether formed in the crystal with *rac*-**3** and w.t. IPPI, as shown in Figure 2B, presumably due to a local disruption in H-bonding of the C-3 OH with Tyr (Phe).

These results have mechanistic implications for IPPI inhibition by the halohydrin phosphoantigens. In the case of **2**, the observation that 3-esters and thioethers form suggests an S_N1 or concerted type of reaction in which protonation plays a role:[8] but with the

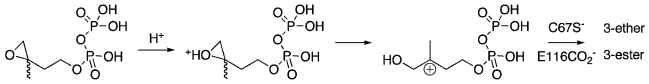

bromohydrins **3**, an S_N2 mechanism is operative, since now the 4-substituted species form:

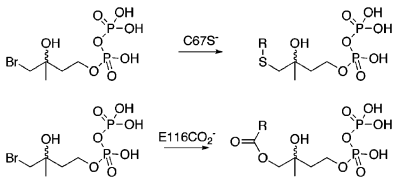

Finally, we investigated the possible interaction of *E*-4-hydroxy-3-methyl-but-2-enyl pyrophosphate (**4**) with IPPI, since **4** is the most potent phosphoantigen known.[13] The crystal structure of **4** bound to IPPI (PDB File 1PPW) is shown in Figure 2C and, expanded, in Figure S5. Again, there are multiple interactions between the diphosphate moiety and Mg^{2+}, K21, K55, R51, and R83, but there is no covalent modification of the protein. Inhibition of IPPI by **4** is only weak ($IC_{50} \approx 50\mu M$, data not shown), clearly ruling out IPPI as a target in $\gamma\delta$ T cell activation by **4**.

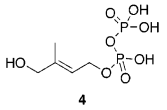

4

Overall, these results are of general interest since they represent the first structural studies of the inhibition of the mevalonate pathway enzyme, IPPI, by the bromohydrin phosphoantigens currently being developed for immunotherapy.[14] Unlike the epoxy pyrophosphates, reaction occurs exclusively at C-4 (not C-3), suggesting an S_N2 reaction for **3** and related halohydrins. The potent phosphoantigen **4** also binds to IPPI, but is a poor inhibitor, clearly indicating a target other than IPPI in $\gamma\delta$ T cell activation.

Acknowledgment. This work was supported by the U.S. Public Health Service (NIH Grants EB00271 and GM50694 to E.O. and AR045504 to C.T.M.). J.W. thanks the Fonds National de la Recherche Scientifique for financial support (IISN grant) and the team at the BM30 synchrotron facilities in Grenoble. Figures were prepared using the VMD program.[15]

Supporting Information Available: Additional experimental results and figures. This material is available free of charge via the Internet at http://pubs.acs.org.

References

(1) Law, M. R.; Wald, N. J.; Rudnicka, A. R. *Br. Med. J.* **2003**, *326*, 1423−1429.
(2) Onyewu, C.; Blankenship, J. R.; Del Poeta, M.; Heitman, J. *Antimicrob. Agents Chemother.* **2003**, *47*, 956−964.
(3) Theriault, R. L. *Expert Rev. Anticancer. Ther.* **2003**, *3*, 157−166.
(4) Kunzmann, V.; Bauer, E.; Feurle, J.; Weissinger, F.; Tony, H. P.; Wilhelm, M. *Blood* **2000**, *96*, 384−392.
(5) (a) Gober, H. J.; Kistowska, M.; Angman, L.; Jeno, P.; Mori, L.; De Libero, G. *J. Exp. Med.* **2003**, *197*, 163−168. (b) Thompson, K.; Rogers, M. J. *J. Bone Miner. Res.* **2004**, *19*, 278−288.
(6) Wilhelm, M.; Kunzmann, V.; Eckstein, S.; Reimer, P.; Weissinger, F.; Ruediger, T.; Tony, H. P. *Blood* **2003**, *102*, 200−206.
(7) Lu, X. J.; Christensen, D. J.; Poulter, C. D. *Biochemistry* **1992**, *31*, 9955−9960.
(8) (a) Wouters, J.; Oudjama, Y.; Barkley, S. J.; Tricot, C.; Stalon, V.; Droogmans, L.; Poulter, C. D. *J. Biol. Chem.* **2003**, *278*, 11903−11908. (b) Wouters, J.; Oudjama, Y.; Stalon, V.; Droogmans, L.; Poulter, C. D. *Proteins: Struct., Funct., Genet.* **2004**, *54*, 216−221.
(9) Durbecq, V.; Sainz, G.; Oudjama, Y.; Clantin, B.; Bompard-Gilles, C.; Tricot, C.; Caillet, J.; Stalon, V.; Droogmans, L.; Villeret, V. *EMBO J.* **2001**, *20*, 1530−1537.
(10) Refinements were performed with the program *SHELXL97* (Sheldrick, G. M.; Schneider, T. R. Direct Methods for Macromolecules. In *Methods in Macromolecular Crystallography*; Turk, D., Johnson, L., Eds.; IOS Press: Amsterdam, 2001; pp 72−81) using the structure of metal-bound IPP isomerase (Protein Data Bank (PDB) reference code 1HX3) as a starting model. Electron density maps were inspected with the graphics program *Turbo-Frodo* (Roussel, A.; Cambillau, C. *Turbo-Frodo*; Biographics, AFMB: Marseille, France, 1992.). Final coordinates have been deposited at the PDB under codes 1PPV, 1X83, 1X84, and 1PPW for *rac*-**3**, *S*-**3**, (Y104F), and **4**-IPPI complex, respectively.
(11) Song, Y.; Zhang, Y.; Wang, H.; Raker, A.; Sanders, J. M.; Broderick, E.; Clark, A.; Morita, C. T.; Oldfield, E. *Bioorg. Med. Chem. Lett.* **2004**, *14*, 4471−4477.
(12) Durisotti, V.; Oudjama, Y.; Wouters, J. Unpublished results.
(13) Hintz, M.; Reichenberg, A.; Altincicek, B.; Bahr, U.; Gschwind, R. M.; Kollas, A. K.; Beck, E.; Wiesner, J.; Eberl, M.; Jomaa, H. *FEBS Lett.* **2001**, *509*, 317−322.
(14) Belmant, C.; Fournié, J.-J.; Bonneville, M.; Peyrat, M. A. Nouveaux Composes Phosphohalohydrines, Procede de Fabrication et Applications. French Patent 2,782,721, March 3, 2000. http://www.innate-pharma.com/.
(15) Humphrey, W.; Dalke, A.; Schulten, K. *J. Mol. Graphics* **1996**, *14*, 33−38.

JA040207I